

Microscopic model for the ablative photodecomposition of polymers by far-ultraviolet radiation (193 nm)

Barbara J. Garrison^{a)}

Department of Chemistry, The Pennsylvania State University, University Park, Pennsylvania 16802

R. Srinivasan

IBM Thomas J. Watson Research Center, Yorktown Heights, New York 10598

(Received 7 November 1983; accepted for publication 16 February 1984)

Short pulses of far-ultraviolet (193 nm) laser radiation are capable of etching organic polymer films without melting the remaining sample. The mechanism proposed for this ablative photodecomposition attributes ablation to the increase in volume that accompanies the photolysis of the polymer. A model of the microscopic process is presented here. The predictions of the model include ablation without melting, a mean perpendicular ejection velocity of 1300 m/s, and an angular distribution of the ablated material which has a narrow peak normal to the surface.

PACS numbers: 79.20.Ds, 81.60.Jw, 82.30.Lp, 82.50. — m

When a pulse (~ 14 ns half-width) of laser radiation of 193-nm wavelength with a fluence above a threshold value falls on a polymer film, the material at the irradiation site is spontaneously etched away to a depth of 1000 Å or more. This process is termed ablative photodecomposition.¹⁻³ Microscopic examination of the surface shows no indication that the substrate has melted or flowed even in the case of polymers with a glass transition temperature as low as 100 °C. Ablative photodecomposition occurs in a variety of organic polymers¹⁻³ at fluences as little as 10 mJ/cm². The process has potential as a "dry" etching step in the semiconductor industry and in certain medical applications.

Why does the 193-nm wavelength radiation cause a neat and clean etch region, while a laser with longer wavelength (~ 500 nm) light melts and damages nearby regions of the sample? At 193 nm the molar extinction coefficient of the material is high ($\sim 10^4$ L mol⁻¹ cm⁻¹) so that 95% of the light is absorbed in the first 3000 Å of the substrate. In addition, the quantum yield for bond breakage is high (between 0.1 and 1), thus the 193 nm light breaks bonds effectively. In contrast, longer wavelength light vibrationally excites the irradiation site. This process can also eventually cause material to desorb from the heated region. The problem still remains, however, after the photochemical bond breakage, of how to explain the ablation of the material from the sample. It has been proposed that since the products of photodecomposition have a larger specific volume than the polymer that they replace, an explosive expansion occurs and there is mass

transport from the sample.³ For example, the specific volume of liquid methylmethacrylate is 30% larger than polymethyl methacrylate (PMMA).⁴

A number of other observations have been made regarding the ablation process. The products that are expelled may be small molecules such as H₂ or CO, fragments of the monomer unit, monomer units and even clusters of the monomer units. There may also be rearrangement or chemical reaction during the ablation process. For example, benzene is formed in fairly high yield from films of poly(ethylene terephthalate), a polymer that contains a phenylene ring but no benzene per se.² The total momentum of the desorbed material has been measured by recoil experiments.⁵ Assuming the average mass of the ablated material is that of a monomer, the mean perpendicular velocity component is 2200 m/s in the case of polyimide. The direction of motion of the ablated material is near normal to the surface.⁵ Finally the etch rate is nearly logarithmic in the laser fluence.^{3,6} The threshold fluence is 10 ± 3 mJ/cm² for PMMA. For a fluence of 100 mJ/cm² the etch depth is ~ 1500 Å per pulse.⁶

We present a microscopic model of this process in order to (i) see if a change in specific volume will lead to ablation without melting, (ii) determine the velocity and angular distributions of the ablated material, and (iii) predict other observables. Briefly, the polymer is approximated by an array of structureless monomer units. Initially all monomer units interact with a potential that makes the sample stable at the polymer density. The photochemical reaction then corresponds to a switch in potential surfaces such that the monomer units now occupy a larger volume. The motion of the

^{a)} Alfred P. Sloan Research Fellow

ensemble of monomer units is followed in time by integrating the classical equations of motion. In the experiment as many as 500 layers of material ablate per laser pulse. Although it is not feasible to include these many monomers in the calculations we do find agreement between the predictions and the experimental results.

The polymer is described by structureless monomer units held together by strong attractive interactions. After the laser light strikes the sample a few of the monomer units react photochemically. We simulate this process by allowing each monomer unit to undergo excitation from an attractive to a repulsive potential surface. This excitation produces a change in the volume that the monomers occupy. For computational simplicity we assume that the polymer is arranged in a face-centered cubic (fcc) crystalline array. This assumption should not significantly affect the conclusion and makes it visually easier to determine the amount of distortion that occurs. The interaction for the bound monomer units is assumed to be pairwise additive with a Lennard-Jones 12-6 form. The interaction between the reacted units and the bound units is described only by the $1/r^{12}$ repulsive term.

The system chosen has the characteristics of PMMA, which has a density of 1.22 g/cc.⁴ Using the monomer mass of PMMA of 100 amu, this density corresponds to a fcc lattice with a lattice constant of 8.1 Å. The arrangement of monomer units is shown in Fig. 1. We assume that the main attractive forces holding the monomer units together are the two carbon-carbon bonds along the chains. The strength of a C-C bond is approximately 3.6 eV. Given the bond strengths and the distance between the units we can determine the Lennard-Jones parameters of the corresponding pair potential. In this case we find that $\epsilon = 0.42$ eV and $\sigma = 5.28$ Å. These parameters yield a cohesive energy for

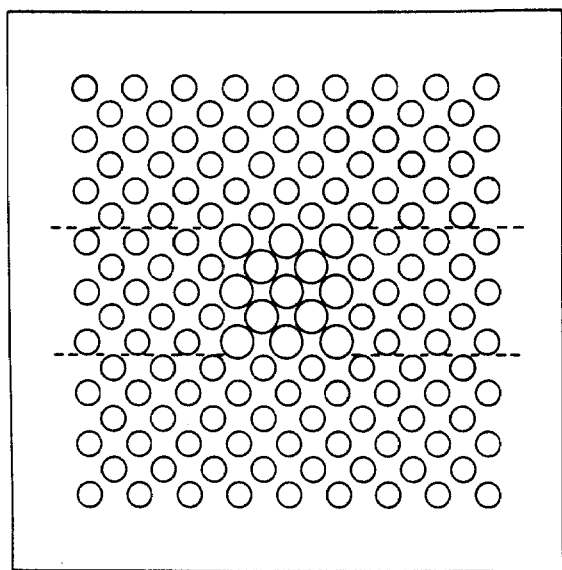


FIG. 1. Surface layer of the ensemble of monomer units. All odd numbered layers have the same configuration of units. The even numbered layers have monomer units in the spaces of the first layer. A total of 10 layers is included in the calculation. The radii are arbitrary although the smaller circles correspond to the polymerized form and the larger circles to the reacted monomers. The two horizontal lines show the region of the space that is graphically displayed in Fig. 2.

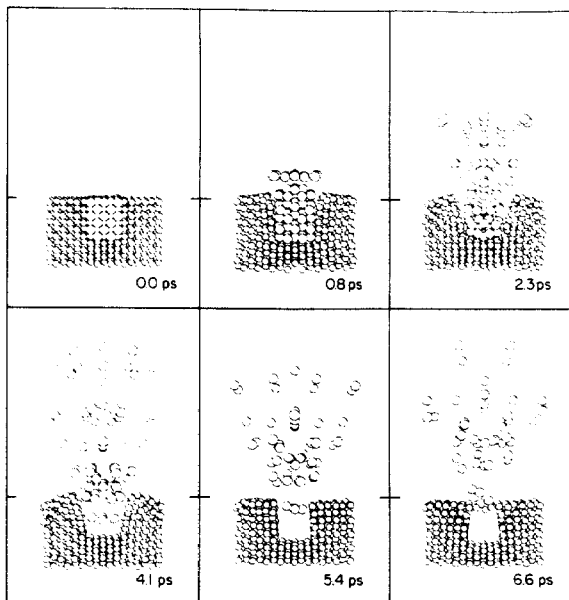


FIG. 2. Movement of the monomers as a function of time. There is a slight perspective in the drawings. The tic marks on the side give the original position of the surface layer.

one monomer unit of 3.6 eV. The coefficient of the $1/r^{12}$ term for the repulsive interaction is chosen so that the cohesive energy of the reacted monomer is 193 nm (6.4 eV) larger than the cohesive energy of the monomer unit in the polymerized form at the same density. This results in a value of 6×10^8 eV Å¹² for the coefficient.

Given the above potentials, Hamilton's classical equations of motion for the particles are integrated in time. As initial conditions we react the central region in the top six layers of the crystal. Due to the fcc symmetry this corresponds to 13 monomers in layers 1, 3, and 5 and 12 monomers in layers 2, 4, and 6 for a total of 75 reacted species.

The results are shown in Fig. 2 where a side view of the inside of the crystal is plotted as a function of time. The reacted monomers are drawn as larger circles. At 0.8 ps the top layer of reacted units begins to ablate. There is some

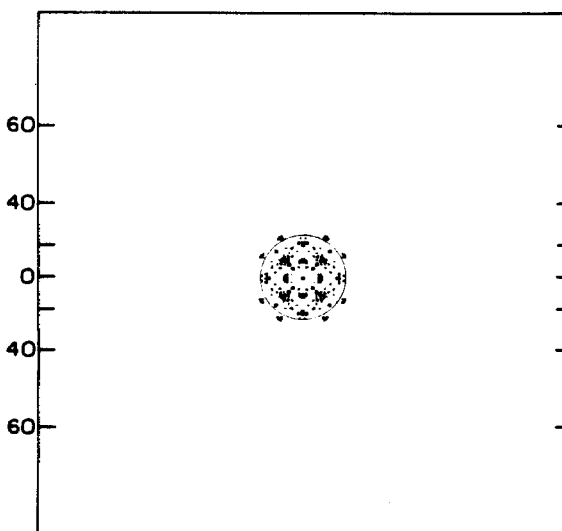


FIG. 3. Angular distribution of the ablated material. See text for a description of the display.

distortion of the crystal at this point. As time progresses more of the reacted monomers leave the crystal with the maximum damage to the crystalline arrangement occurring at 4 ps. At 6 ps, however, the crystal has annealed to some extent. An interesting artifact of the calculation is that the sides of the crystal undergo a vibrational oscillation. (Compare the width of the pit at 4 and 6 ps.) Rather than this oscillation in the experiment, we would expect there would be an outgoing shockwave originating from the ablated region. The important conclusion is that this model predicts ablation without melting. It is conceivable that the impact of the explosion could have spread sideways and significantly damaged the crystal.

After 6 ps the total kinetic energy of the ablated material is 102 eV so that the average energy is 1.4 eV per monomer. The mean perpendicular velocity is 1300 ± 300 m/s, if the first layer of ejected material is not included. These numbers are in agreement with the experimental values especially since (a) the experimental values are measured by momentum recoil and an average mass must be assumed⁵ and (b) we have made no attempt to fit the ejection velocity by adjusting the parameters describing the repulsive potential. By carefully analyzing the 0-ps and 6-ps frames of Fig. 2 we find that our crystal recoils by approximately one-half a layer spacing.

The angular distribution of the ablated material is shown in Fig. 3. In this display each monomer is plotted on a flat-plate collector an arbitrary distance above the crystal. The radial distance of a plotted point from the center of the plate is proportional to the polar angle of ejection. The circle is drawn at a distance that corresponds to an angle of 25° from the surface normal. The calculations predict the distribution to be extremely narrow and peaked in the direction perpendicular to the surface in agreement with the experimental results.⁵ It appears that the walls of the pit channel the ablated material into the upward direction. The display in Fig. 3 is on the same scale as comparable plots of angular distributions from ion bombardment simulations. In the latter case, however, the distributions from both experiment and calculations extend to over 60° from the surface normal.⁷⁻⁹ Thus the physical process (not the specific crystal structure) controls the angular distribution.

One of the goals of this study is to understand the origin of the fluence threshold for ablation. Various schemes where only a fraction of the 75 monomers in the central region are allowed to react were tested. If the 12 monomers in layers 2 and 4 are reacted, the calculation predicts that all of the reacted species as well as the 9 central ones in the first layer and the 5 central ones in the third layer ablate. The ones that did not eject were near the edges of the irradiated region and still felt the attractive forces to the walls. The 9 first layer monomers as well as the 5 third layer monomers eject as intact units. Thus the volume explosion is strong enough to expel pieces larger than a monomer unit. If only the 13 mon-

omers in the third layer are photolyzed nothing ablates, although there is upward motion of monomers above the photolyzed ones.

This model presents a qualitative picture of how material ablates. As seen from Fig. 2, and by examining the calculations in detail, the material ablates layer by layer with the first layer ejecting in less than 1 ps and the sixth layer taking almost 6 ps. The sixth layer is 20 Å below the surface. If there were no obstructions, a monomer traveling at 1300 m/s should take only 1.5 ps to reach the surface so that there is a time delay for the material deeper in the sample to ablate. However, there does not appear to be any sideways motion in this delay period. A highly desirable experiment would be the analysis of the ablated material as a function of time in order to observe the possible changes in composition. Alternatively one can assume that the calculations give the proper time sequence for the ablation of the various layers. If we assume that each photon breaks a bond, then by Beer's law the material in the top layers of the sample should be broken into the smaller fragments. The material from deeper in the sample should consist of monomer and larger species. Thus, by measuring a mass spectrum of the ejected material a correlation to its original position in the sample can be made.

In conclusion, a microscopic model for the ablative photodecomposition of polymer films that makes specific predictions is presented. The basis of the model is a volume change of the material after the photolysis induced by the far UV radiation. The predictions of the model are as follows. (1) The reacted material ablates without melting the remainder of the sample. (2) The average perpendicular velocity of the ejected material is ~ 1300 m/s. (3) The angular spread is small and peaked in the direction normal to the surface. (4) The material ablates layer by layer.

Partial support for these studies is gratefully acknowledged from the Office of Naval Research and the National Science Foundation. B.J.G. also thanks the Alfred P. Sloan Foundation for a research fellowship and the Camille and Henry Dreyfus Foundation for a grant for newly appointed young faculty. We are especially indebted to J. P. Heicklen for his encouragement in this collaborative effort.

¹R. Srinivasan and V. Mayne-Banton, *Appl. Phys. Lett.* **41**, 576 (1982); J. E. Andrew, P. E. Dyer, D. Forster, and P. H. Key, *Appl. Phys. Lett.* **43**, 717 (1983).

²R. Srinivasan and W. J. Leigh, *J. Am. Chem. Soc.* **104**, 6784 (1982).

³R. Srinivasan, *J. Vac. Sci. Tech. B* **4**, 923 (1983).

⁴*Encyclopedia of Polymer Science and Technology* (Interscience, New York, 1964), Vols. 3-4.

⁵Shu-Huei Liu and R. Srinivasan (unpublished).

⁶R. Srinivasan and B. Braren, *J. Polymer. Sci.* (in press).

⁷N. Winograd, B. J. Garrison, and D. E. Harrison, Jr., *Phys. Rev. Lett.* **41**, 1120 (1978).

⁸R. A. Gibbs, S. P. Holland, K. E. Foley, B. J. Garrison, and N. Winograd, *J. Chem. Phys.* **76**, 684 (1982).

⁹B. J. Garrison, *J. Am. Chem. Soc.* **105**, 373 (1983).